Effect of the corrosion of plate with double cracks in bonded composite repair

Mohamed Berrahou[*], Mokadem Salem[a], B. Mechab and B. Bachir Bouiadjra[b]

LMPM, Department of Mechanical Engineering, University of Sidi Bel Abbes, BP 89 Cité Ben M'hidi 22000, Sidi Bel Abbes, Algeria

Abstract. This paper presents a three-dimensional finite element method analysis of repairing plate with bonded composite patch subjected to tensile load. The effect of the corrosion on the damage of the adhesive (FM73) in the length of two horizontal cracks on the both sides is presented. The obtained results show that the crack on the left side creates a very extensive area of the damaged zone and gives values of the stress intensity factor (SIF) higher than that on the right side. We can conclude that the left crack is more harmful (dangerous) than that on the right side.

Keywords: repairing plate; composite; FEM; fracture mechanics; corrosion

1. Introduction

The cracks can occur in many structural components of plates form. They are the cause of premature damage in structures. The stress intensity factor can be taken as an essential parameter to analyze crack (Cao and Liu 2012, Cetisli and Kaman 2014). Advanced composite technology has been widely used for several years to reinforce metallic structures in aerospace applications. One of the resulting technologies is the bonded patch, which is now, in some sense, finding applications in other areas such as civil engineering (Salem *et al.* 2015, Mechab *et al.* 2016, Serier *et al.* 2016).

Several numerical researches were performed to analyse the performance of the Boron /Epoxy repair. Tay *et al.* (1996) analysed the effect of the Boron/Epoxy patch on the rigidity of the aircraft metallic structures. They showed that this rigidity was highly improved by the presence of the Boron/Epoxy patch repair or reinforcement. Ouinas *et al.* (2007) made a comparison between the Boron/Epoxy and Carbon/ Epoxy for repairing aircraft structures. They showed that the Boron/Epoxy reduction of the stress intensity factor at the crack tip is more significant by the use of the Boron/Epoxy. In addition, the thermal residual stresses due to the adhesive curing are less significant for the Boron/Epoxy patch. Several authors (Mhamdia *et al.* 2012, Albedah *et al.* 2011, Benyahia *et al.* 2014) showed that the stress intensity factor for patched crack exhibits an asymptotic behaviour as the crack length increases. This is due to the stress transfer toward the composite patch throughout the adhesive layer.

The technology involves adhesively bonding patches of advanced fiber composite materials to repair damaged aircraft structures and to stop stress corrosion cracking (Berrahou and Bachir Bouiadjra 2016). The repairs are structurally very efficient, can be applied rapidly and are cost effective. The technology has many advantages over traditional mechanical repair methods, such as bolting or riveting. Composite patches are lighter, offer more uniform load transfer, seal interfaces reducing corrosion and leakage, create minimal damage to the parent structure and facilitate non-destructive inspections.

Corrosion and fatigue are the major factors that contribute to the aging of aircraft (Schubbe *et al.* 2016, Hosseini-Toudeshky *et al.* 2012). During its service life, an aircraft is subjected to severe structural and aerodynamic loads which may result from repeated landing sand take-off, fatigue, Ground handling, bird strikes and environmental degradation such as stress corrosion, which cause damage or weakening of the structure. A repair or reinforcement of the structure to restore the structural efficiency and thus assure the continued airworthiness of the aircraft has become an important issue in recent years.

Bouanani *et al.* (2013) has estimated of the adhesive damage and failure in bonded composite repair of aircraft structures using modified damage zone theory .and there are shows that adhesive damage is principally located at the free edges of the patch and over crack region. Benyahia *et al.* (2014) analyzed four different shapes (rectangular, trapezoidal, circular and elliptical) showed, the rectangular patch offers high safety compared to the other patch shapes but it reduces the repair performances. The elliptical patch can be considered as the optimal shape because it simultaneously improves the repair efficiency and the repair durability.

In this study, a three-dimensional finite element method is used to analyze the effect of the corrosion on the damage of the FM73 epoxy adhesive of bonded composite repair of aircraft structures. The effects of length of two horizontal cracks on the both sides of corrosion are presented.

∗Corresponding author, Professor
  E-mail: berrahou22@yahoo.com
[a]Ph.D.
  E-mail: moka_salem@yahoo.fr
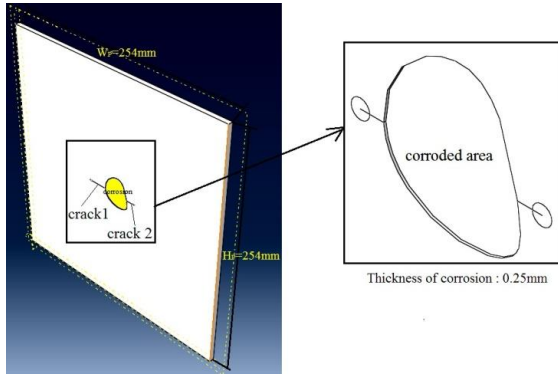[b]Ph.D.
  E-mail: bachirbou@yahoo.fr

Fig. 1 Geometrical model

Table 1 Elastic properties of different

	Aluminium 2024-T3	Boron/ Epoxy	Adhesive (FM-73)
Longitudinal Young's Modulus E_1 (GPa)	72	200	4.2
Transversal Young's Modulus E_2 (GPa)		19.6	
Transversal Young's Modulus E_3 (GPa)		19.6	
Longitudinal Shear Modulus G_{12} (GPa)		7.2	
Transversal Shear Modulus G_{13} (GPa)		5.5	
Transversal Shear Modulus G_{23} (GPa)		5.5	
Longitudinal Poisson Ratio v_{12}	0.33	0.3	0.32
Transversal Poisson Ratio v_{13}		0.28	
Transversal Poisson Ratio v_{23}		0.28	

2. Geometrical and FE models

The geometrical model of the structure considered in this study is shown in Fig. 1. Consider an aluminum 2024-T3 plate characterized by its height H_P=254 mm, width W_p=254 mm and thickness e_p=5 mm with random corrosion. The plate has two cracks of length a on each side of the corrosion repaired by a simple Boron- Epoxy patch of dimensions H_r=75 mm, W_r=130 mm and e_r=2 mm. The plies in the patch had unidirectional lay-up where the fibers are oriented along the specimen length direction (parallel to the direction of load). The patch being bonded to the plate by an FM 73 adhesive of thickness 0.15 mm. The plate is subjected to a mechanical loading of amplitude 100 MPa. The mechanical properties of the patch plate and of the adhesive are shown in Table 1.

The geometric shape of the corrosion used is randomly in 3D with a thickness 0.25 mm, before repairing the structure, the corroded area is cleaned to remove the Corrosion film and keep the same mechanical properties.

The analysis of the shear stresses of the adhesive in this study it's very important, because the intensity of these stresses determines the risk of adhesion failure. In the following, the distribution of the shear stresses of the adhesive in the plane *xy*, *xz* and *yz* (τ_{xy}, τ_{xz}, and τ_{yz}) is
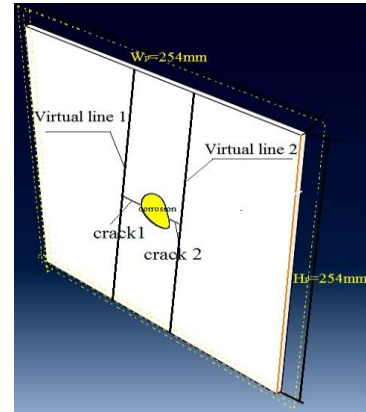

Fig. 2 Representation of the virtual line of stress variations in the adhesive layer

presented along a virtual line tangent to the crack tip Fig. 2.

The analysis involves a three-dimensional finite element method by using the commercially available finite element code ABAQUS (2007). The finite element model consisted of three subsections to model with corrosion, the adhesive, and the composite patch. The procedure used in the finite element analysis is as follow: the tensile stress was applied to the gripped specimen. General static "STEP" -option was used for analysis with ABAQUS. Automatic increment of step was used with maximum number of increments of 200. Minimum increment size was 10^{-5}. Maximum increment size was one. Nevertheless, the ABAQUS solver code could override matrix solver choice according to the "STEP" -option.

The finite element model consisted of three subsections to model the cracked plate, the adhesive, and the composite patch. The model consisted of 85179 quadratic hexahedral elements having 99 quadratic wedge elements and total number of 85296 degrees of freedom: 67448 in the plate, 4462 in the adhesive layer, and 8924 in the patch. The aluminium plate had three layers of elements in the thickness direction, the adhesive had only one layer of elements through thickness and the patch had two layers of elements through thickness. However, to generate crack front some brick elements are replaced by "crack-blocks". These crack-blocks are meshes of brick elements, which are mapped into the original element space and merged with surrounding mesh. The mesh was refined near the crack tip area with an element dimension of 0.05 mm using at least fifteen such fine elements in the front and back of the crack front. Fig. 3(a) present the mesh refinement in the crack tip region and Fig. 3(b) shows the overall mesh of the specimen. The Stress intensity factor (SIF) at the crack front was extracted using the virtual crack closure technique (VCCT).

The VCCT is based on the energy balance proposed by Irwin. In this technique, SIF are obtained for the three fracture modes from the equation

$$J_e = \frac{K_i^2}{E} \qquad (1)$$

Where J_e is the energy release rate for mode *I*, K_i is the stress intensity factor for mode *I*, *E* is the elastic modulus.
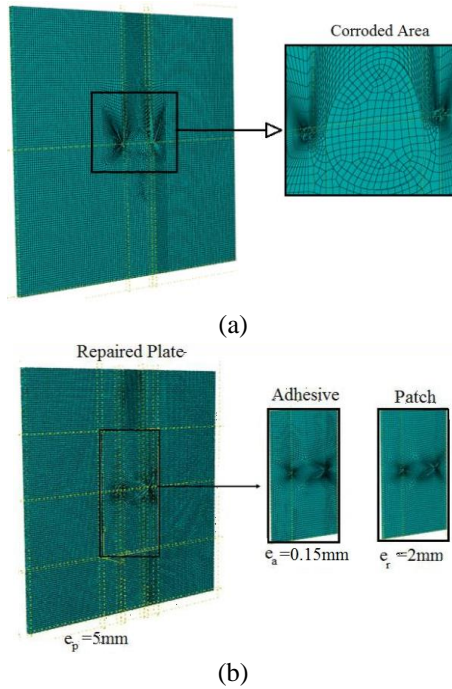
(a)

(b)

Fig. 3 (a) Mesh of the corroded plate, (b) A typical finite element (FE) for a global mesh model

(a)   (b)   (c)

Fig. 4 Damage zones for rectangular patch shape for different length of crack. (a) a=5 mm, (b) a =10 mm et (c) a=20 mm

Fig. 5 Damage ratio for different value of length of crack

The structure is modeled by cubic elements of eight nodes. The mesh used in the model of finite elements is represented in Fig. 3. The rectangular shape of the composite patch can be identified in this figure. A regular mesh is made for the whole structure. This mesh remains the same throughout the calculation. The perfect bonding is created between the plate and the composite patch by merging the nodes of the elements. Merging the nodes results in having the same mesh for the structure and for the composite patch. Therefore, a refined mesh is made around cracks and corrosion. The total number of elements of the structure is 29200. The size of the side of an element away from the crack is equal to 0.015 mm for the whole structure and 0.004 mm in the vicinity of the crack.

3. Results and discussion

This criterion is satisfied when the maximum principal strain in the material reaches the ultimate principal strain. For each failure criterion an ultimate strain will be defined and the corresponding damage zone size at failure determined.

Under damage zone theory, we assume that the adhesive joint fails when the damage zone reaches a certain reference value. The damage zone can be defined by either the stress or the strain criterion. The strain criterion is more appropriate when the adhesive exhibits significant nonlinearity. There are two modes of failure relevant to the adhesive joints: interfacial and cohesive failure. In the interfacial mode, the failure load of the adhesive joint depends on the interfacial stress near the interfaces between the adhesive and the adherend Ban Chang *et al.* (2008). However, the adhesive fails when cohesive failure occurs in
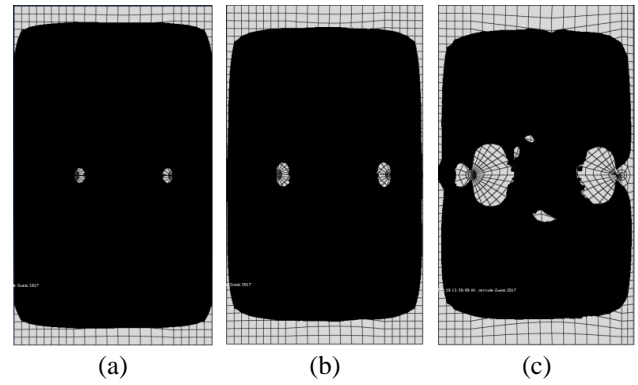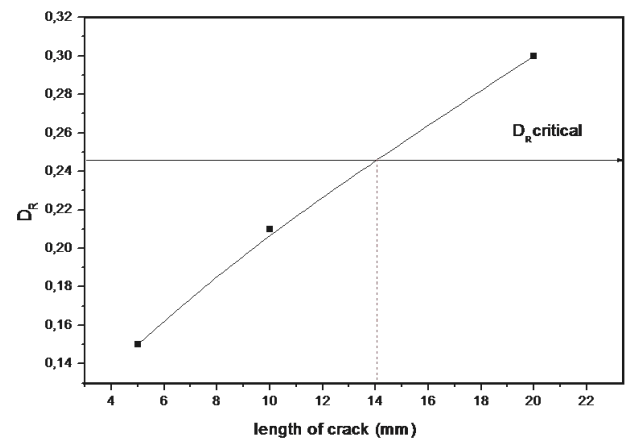
the joint. Since cohesive failures certainly occurred in the adhesive joint, we recommend using the adhesive failure criterion for the damage zone. The failure criterion, for isotropic materials, such as the Von-Mises and Tresca criteria can be used to better understand adhesive failures. We can also predict the failure of the adhesive joints by using the damage zone ratio method. The damage zone ratio D_R is defined as follow

$$D_R = \frac{\sum A_i}{l.w} \qquad (2)$$

D_R is the damage zone ratio, A_i the area over which the equivalent strain exceeds 7.87% (ultimate strain for the FM 73 Adhesive). It was shown that the FM 73 adhesive fails when the D_R value reached the critical value (D_{Rc}=0.2474) Ban Chang *et al.* (2008).

The damage zone theory was used to evaluate the damage evolution in the adhesive layer. The area of damaged zone is presented in grey color.

One of the main geometric features of the crack is its size. Its influence on crack propagation criteria in a mode I cracked plate (horizontal crack) repaired by composite patch was analysed numerically. The Figs. 4, 5 and 6 show the effect of the size of the crack on the evolution of the damaged area repaired by the patch. Then the stress intensity factor is calculated to compare the evolution of D_R.
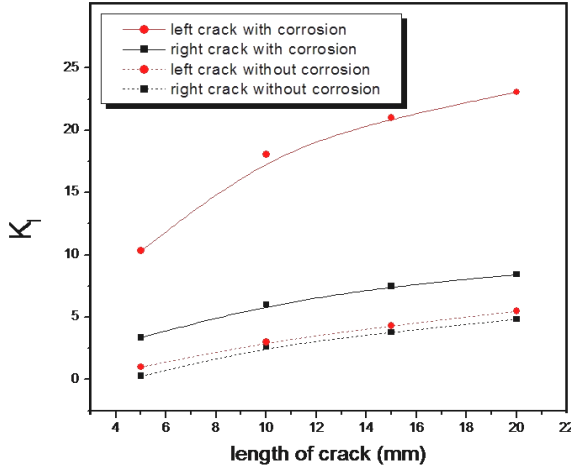
Fig. 6 Variation of the stress intensity factor for different value of length of crack

3.1 Effect of the crack length

To see the effect of the crack length on the extent of the damaged zone of the adhesive, Fig. 4 shows the distribution of the damaged area in the adhesive joint for different crack sizes. From this figure, it can be seen that the increase in the length of crack causes an increase of the damaged area surrounding the crack and at the edge of the patch for all the crack sizes. For the crack size of (a=20 mm) it is noted that the damaged surface affects all the sides of the patch, and there are also damaged areas on the left side of the corrosion.

3.2 Effect of crack length on damage ratio

The ratio of the damaged zone D_R is analysed in Fig. 5. It represents the curve of the variation of the values of the ratio of the damaged area D_R as a function of the variation in the length of cracks. The increase in the D_R value is due to the increase in crack length. It should be noted that the critical value of the ratio D_R is reached when (a_{right}=a_{left}) ≈14 mm shown in Fig. 5. The maximum value of D_R is observed for (a_{right}=a_{left})=20 mm.

3.3 Effect of crack length on the SIF.

The effect of the length of the crack on both sides of the corrosion on the variations of the stress intensity factor K_I is shown in Fig. 6. Whatever the side of the crack propagation (left or right), It is found that the values of the K_I factor increase in the crack size. The results clearly show that the crack on the right side has lower K_I values than those on the left side. Indeed, the reduction of the SIF for the crack on the right side can be estimated at 60% with respect to that on the left side whatever the length of the crack. The increase of the SIF is of the order of 65% when the crack increases from 5 mm to 20 mm on the right side and is about 55% on the left side.

In Fig. 6 we present the variation of the SIF in the left and the right crack tips for cracks emanating for corrosion and cracks initiated in non-corroded plate. We can note that
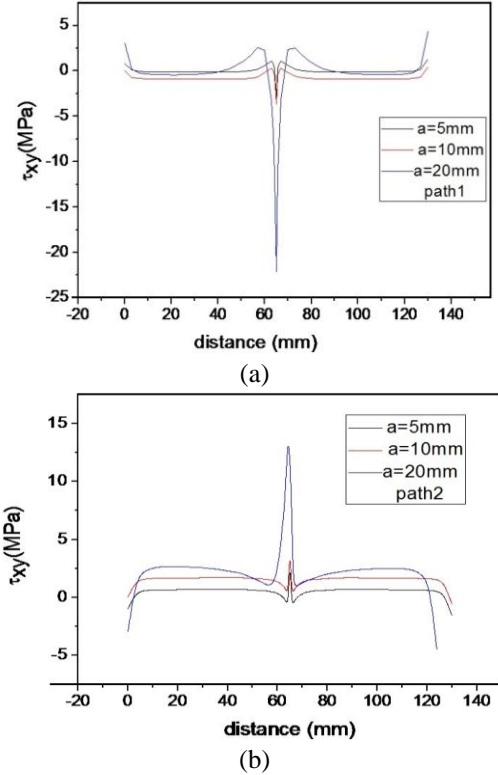

(a)

(b)

Fig. 7 Variation of the shear stress τ_{xy} in the adhesive layer. (a) for left crack, (b) for right crack

the crack emanating from corrosion present higher stress intensity factors which allow us to deduce that this type of crack is most dangerous.

The stress crack intensity factor of the left crack is higher because the area of overlap in the right region is less significant, so the transfer of stress from the right crack is less significant it can be seen that in Fig. 4(c). It is noted that the damaged zones form on the left side of the corrosion while on the right side no appearance which leads to lower values of SIF, and also the form of corrosion is not symmetrical. This behavior is confirmed Fig. 6 where the K_I on the left side is larger than that on the right side, which induces larger damaged zones at the level of the left crack.

3.4 Stress distribution in the adhesive layer

Glue is a fundamental element, its main role is to ensure a good adhesion and minimize the transfer of stresses from the structure of the composite patch. Knowledge of the stress intensities and their distribution in the adhesive layer is of great importance in predicting the lifetime of the repaired structure. It is for these reasons the study was analysed numerically by the finite element method the distribution of stresses in the adhesive layer. The influence of the crack size is demonstrated on the variations of the shear stresses in the adhesive layer. These stresses are traced along two imaginary lines that pass through the crack tips towards the edges of the patch (superior and inferior).

The influence of crack size of shear stress variations in the *xy,* *xz* and *yz* planes is shown in Figs. 7, 8 and 9 for an applied load σ=100 MPa (E_{ad}=4200 MPa et e_{ad}=0.15 mm).

(a)

(b)

Fig. 8 Variation of the shear stress τ_{xz} in the adhesive layer. (a) for left crack, (b) for right crack
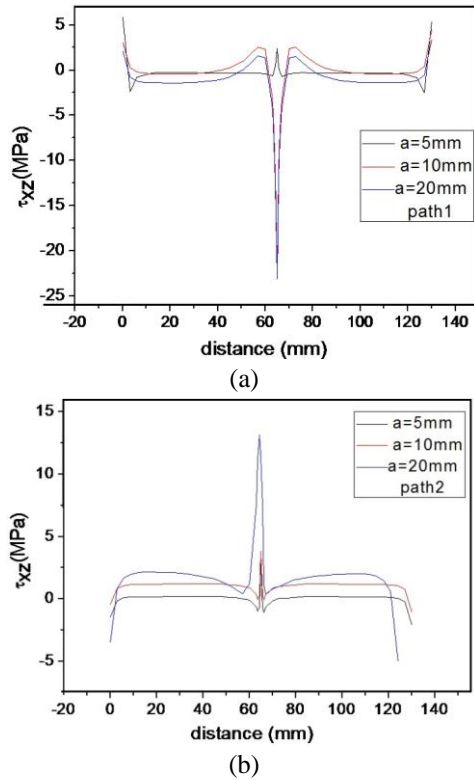

(a)

(b)

Fig. 9 Variation of the shear stress τ_{yz} in the adhesive layer. (a) for left crack, (b) for right crack

Figs. 7 and 8 represent the distribution of shear stresses τ_{xy} and τ_{xz} in the adhesive layer for different crack sizes. It is noted that the stresses τ_{xy} and τ_{xz} increase with the increase of the crack size and are maximal at the points of cracking left and right side.

From these figures it can be seen that the values of the constraints on the left side are higher than those on the right side, this observation is similar to that observed in the results obtained in Figs. 4 and 6. It is observed that the stresses have an opposite behaviour in signs where the values on the left side are negative on the right side are positive.

The shear stresses τ_{yz} (Fig. 9) are maximal at the edges of the patch in the intervals ($0 < H_{ad} < 10$ mm) and (120 mm $< H_{ad} < 130$ mm) and vanish between 10 mm and 120 mm. There is a similarity in behaviour for both sides.

4. Conclusions

This work was part of a global approach to understanding the corrosion behaviour of aluminium alloys of the 2000 series. The work focused in particular on the aluminium alloy 2024.The results are obtained using the finite element method of a corroded plate with two horizontal cracks on both sides of the corrosion, repaired with composite. The behavior of the stress intensity factor and the distribution of the damaged areas in the adhesive, made it possible to deduce the following conclusions.

• The increase of the crack length leads to an increase of the damaged zone in the vicinity of the crack and to the
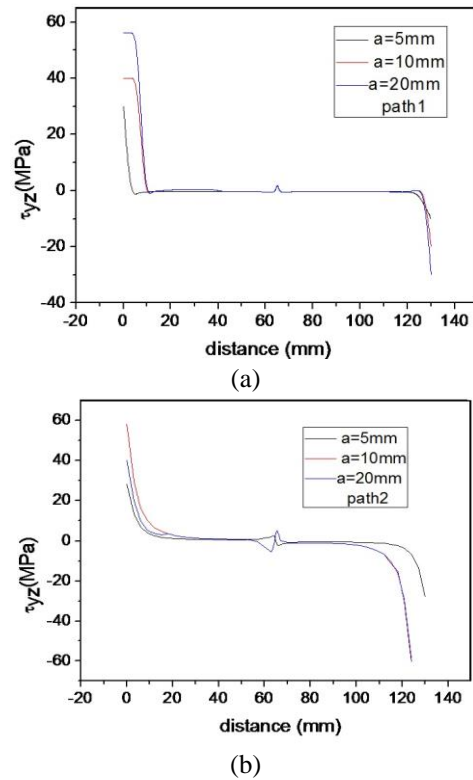
edge of the patch, and it is noted that the critical value of the D_{Rc} ratio is reached when ($a_{right} = a_{left}) \approx 14$ mm.
• It is found that the K_I values increase with the crack size and clearly show that the crack on the right side has low K_I values compared to those on the left side.
• The stresses τ_{xy} and τ_{xz} increase with the increase of the crack size and are maximal at the left and right crack tips. One observes that the constraints have an opposite behavior where the values on the left side are negative. On the other hand, they are positive.

References

Abaqus (2007), ABAQUS Standard/User's Manual, Version 6.11. Hibbit Karlsson & Sorensen, Inc., Pawtucket, RI, USA.

Albedah, A., Bachir Bouiadjra, B.B., Mhamdia, R., Benyahia, F. and Es-Saheb, M. (2011), "Comparison between double and single sided bonded composite repair with circular shape", *Mater. Des*., **32**, 996-1000.

Ban, C.S., Lee, Y.H., Choi, J.H. and Kweon, J.H. (2008), "Strength prediction of adhesive joints using the modified damage zone theory", *Compos. Struct*., **86**, 96-100.

Benyahia, F., Albedah, A. and Bachir Bouiadjra, B.B. (2014), "Analysis of the adhesive damage for different patch shapes in bonded composite repair of aircraft structures", *Mater. Des*., **54**, 18-24.

Benyahia, F., Albedah, A. and Bachir Bouiadjra, B.B. (2014), (2014), "Elliptical and circular bonded composite repair under mechanical and thermal loading in aircraft structures", *Mater. Res*., **17**, 1219-1225.

Berrahou, M. and Bachir Bouiadjra, B.B. (2016), "Analysis of the

adhesive damage for different patch shapes in bonded composite repair of corroded aluminum plate", *Struct. Eng. Mech.*, **59**(1), 123-132.

Bouanani, M.F., Benyahia, F., Albedah, A., Aid, A., Bouiadjra, B.B., Belhouari, M. and Achour, T. (2013), "Analysis of the adhesive failure in bonded composite repair of aircraft structures using modified damage zone theory", *Mater. Des.*, **50**, 433-439.

Cao, Z. and Liu, Y. (2012), "A new numerical modeling for evaluating the stress intensity factors in 3-D fracture analysis", *Struct. Eng. Mech.*, **43**(3), 321-336.

Cetisli, F. and Kaman, M.O. (2014), "Numerical analysis of interface crack problem in composite plates jointed with composite patch", *Steel Compos. Struct.*, **16**(2), 203-220.

Hosseini-Toudeshky, H., Ghaffari, M.A. and Mohammadi, B. (2012), "Finite element fatigue propagation of induced cracks by stiffeners in repaired panels with composite patches", *Compos. Struct.*, **94**, 1771-1780.

Mechab, B., Chama, M., Kaddouri, K. and Slimani, D. (2016), "Probabilistic elastic-plastic analysis of repaired cracks with bonded composite patch", *Steel Compos. Struct.*, **20**(6), 1173-1182.

Mhamdia, R., Serier, B., Bachir Bouiadjra, B.B. and Belhouari, M. (2012), "Numerical analysis of the patch shape effects on the performances of bonded composite repair in aircraft structures", *Compos*: *Part B*, **43**, 391-397.

Ouinas, D., Bachir Bouiadjra, B.B., Serier, B. and Said Bekkouche, M. (2007), "The effects of disbonds on the stress intensity factor of aluminium panels repaired using composite materials", *Compos. Struct.*, **78**, 278-284.

Salem, M., Bachir Bouiadjra, B.B., Mechab, B. and Kaddouri, K. (2015), "Elastic-plastic analysis of the *J* integral for repaired cracks in plates", *Adv. Mater. Res.*, **4**(2), 87-96.

Schubbe, J.J., Bolstad, S.H. and Reyes, S. (2016), "Fatigue crack growth behavior of aerospace and ship-grade aluminum repaired with composite patches in a corrosive environment", *Compos. Struct.*, **144**, 44-56.

Serier, N., Mechab, B., Mhamdia, R. and Serier, B. (2016), "A new formulation of the J integral of bonded composite repair in aircraft structures", *Struct. Eng. Mech.*, **58**(5), 745-755.

Tay, T.E. and Chau, F. (1996), "Bonded boron-epoxy composite repair and reinforcement of cracked aluminium structures", *Compos. Struct.*, **34**, 339-347.

CC